Waveguide surface plasmon resonance studies of surface reactions on gold electrodes

J. C. Abanulo,[ab] R. D. Harris,†[a] A. K. Sheridan,[a] J. S. Wilkinson[a] and P. N. Bartlett*[b]

[a] *Optoelectronics Research Centre, University of Southampton, Southampton, UK SO17 1BJ*
[b] *Department of Chemistry, University of Southampton, Southampton, UK SO17 1BJ*

Received 14th December 2001, Accepted 14th December 2001
First published as an Advance Article on the web 23rd May 2002

We describe the fabrication and characterisation of gold-coated graded index channel waveguide sensors designed for simultaneous electrochemical and surface plasmon resonance studies. The active sensing electrode area is a thin gold film between 0.5 and 5 mm in length and 200 μm wide deposited on top of a 3 μm wide waveguide which forms one arm of a Y-junction while the other arm of the Y-junction serves as a reference. Using these devices we have measured simultaneously the changes in transmittance through the device whilst carrying out cyclic voltammetry in either sulfuric or perchloric acid solution or during the deposition of an UPD layer of copper at the gold surface. In all cases we obtain stable and reproducible results which demonstrate the very high sensitivity of the devices to sub-monolayer changes occurring at the gold electrode surface. The response of these integrated optoelectrochemical devices is discussed in terms of a numerical model for the propagation of light within the waveguide structure.

Introduction

A surface plasmon is a collective oscillation of free electrons which propagates along the surface of a metal with the magnetic field vector parallel to the metal surface (it is a TM- or p-polarised wave).[1] To allow propagation of a surface plasmon, a metal having negative dielectric permittivity of magnitude greater than that of the bounding dielectric at the wavelength of operation is required. The principal component of the electric vector of the surface plasmon is perpendicular to the metal surface and the fields decay exponentially, and rapidly, from the interface into both the metal and the contacting superstrate. As a consequence the surface plasmon is very sensitive to changes in the real and imaginary components of the refractive index at the metal surface and in the superstrate close to (within about 300 nm) the metal surface. Surface plasmon resonance (SPR) describes a collection of related techniques which exploit this high surface sensitivity. In SPR experiments, surface plasmons are resonantly excited at the metal surface by matching the component of the wavevector of the incident light parallel to the interface to the surface plasmon wavevector. Under this condition a significant proportion of the incident power is coupled into the high loss surface plasmon, leading to a significant increase in the optical attenuation of the reflected

† Present address: Marconi Optical Components Ltd., Caswell, Towcester, Northants, UK NN12 8EQ.

beam. The matching of the wavevectors of the incident light and the surface plasmon can be achieved by varying the angle of incidence of the incident light on the interface, by varying the wavelength of the incident light at a constant angle of incidence, or by varying the wavevector of the surface plasmon itself by altering the refractive index of the superstrate medium.

SPR techniques can be divided into those which use prisms, those which use grating couplers, and those which use integrated optical waveguide structures. A commonly used arrangement to employ SPR is the Kretschmann configuration[1] in which the metal is deposited as a thin evaporated film, typically 30 to 60 nm thick, on the base of a prism. In this configuration the incident p-polarised light excites the surface plasmon in the metal overlayer through its evanescent field resulting in frustrated total internal reflection. The resonant condition is detected by a reduction in the intensity of the light reflected from the base of the prism as a function of the angle of incidence. If a CCD detector is used, the intensity of the reflected light at a range of incident angles can be recorded simultaneously[2] or an SPR image of the surface can be recorded.[3] The Otto configuration is a closely related method in which the high index prism is placed within 500 to 1000 nm of the metal/superstrate interface, the choice of distance depending on the wavelength of the incident light and the refractive indices of the metal and the medium.

In grating coupler methods the prism is replaced with a substrate of dielectric material, such as glass, with a grating etched on its surface, and with the metal film deposited on the grating. At resonance, the *k*-vector of the grating matches the difference between the wavevector of the surface plasmon and the parallel component of the wavevector of the incident radiation, removing the need for a prism to achieve phase-matching.

In integrated optical waveguide SPR structures the incident light propagates along a waveguide on top of which the thin metal film is deposited.[4] For the transverse magnetically (TM- or p-) polarized mode the principal component of the magnetic field is parallel to the substrate and waveguide surface and normal to the direction of propagation while the principal component of the electric field is normal to the substrate, and metal, surface. When the wavevector of the waveguide mode closely matches that of the surface plasmon, the coupling of light into the surface plasmon is observed as a drop in the intensity of the TM-polarized light emerging from the end of the waveguide. The refractive indices of the materials on both sides of the metal film (the waveguide substrate and the superstrate), and the thickness and permittivity of the metal, as well as the wavelength, affect the strength of coupling between the light propagating in the waveguide and the surface plasmon, and the position of the resonance. Near the resonance condition small changes in the complex refractive index of the superstrate within about 300 nm of the metal surface produce large changes in the attenuation in the intensity of the light transmitted through the waveguide. The waveguide approach to SPR measurement has a number of advantages. There is no need for bulk optical components and accurate angle measurement as required in the prism method. In addition the sensing areas can be small (of the order of 5 μm by 1 mm) and the method lends itself to integration and multichannel measurements.

Over recent years SPR devices have been commercially exploited and widely applied to biosensing applications[3,5,6] taking advantage of the high surface sensitivity of the technique. Typically these applications use thin evaporated gold films coated with selective chemistries to detect the binding or reaction of target analytes from solution. In these applications no attempt is made to control the potential of the gold surface with respect to the contacting electrolyte solution.

SPR techniques have been used in combination with electrochemistry to study processes at electrode surfaces by a number of authors dating back to the late 1970s. For example, Chao *et al.*[7] used SPR in the Kretschmann configuration, and ellipsometry, to study the electrochemistry of gold in sulfuric acid. At the same time Kolb *et al.*[8] used the Kretschmann configuration to investigate the effects of the electrode potential in the double layer region on the surface plasmon frequency for gold and silver electrodes in perchlorate solution. Gordon and Ernst[9] also used the Kretschmann configuration to study surface plasmons on silver electrodes in contact with aqueous perchlorate and halide solutions. More recently Iwasaki *et al.*[10] have used the Kretschmann configuration to study (111) oriented gold films and electrode reactions at gold surfaces[11,12] and it has been used to study redox transformations in electroactive polymers at electrode surfaces.[13,14] The Kretschmann configuration has the disadvantage that it is limited to the study of thin evaporated metal films; to overcome this problem Tadjeddine *et al.*[15,16] have used the Otto configuration which allows single crystal metal surfaces to be used, albeit at the expense of additional experimental

difficulties. All of these studies have demonstrated that the SPR technique is very sensitive to changes occurring at the electrode surface.

An increasing number of studies, starting with the work of Itoh and Fujishima,[17] have recognized the power of combining electrochemistry with planar waveguide structures, although to date the larger proportion of these have concentrated on the use of planar waveguides coated with a transparent electrode made from a conducting tin oxide film.[18–24] In this configuration the planar waveguide behaves as an attenuated total reflection (ATR) structure in which the evanescent wave at the waveguide surface is used to measure the absorption of light by species present in solution within a couple of hundred nanometres of the electrode surface. If the waveguide is carefully designed it is possible to achieve very high sensitivity. When used in this way the waveguide structure responds to changes in the imaginary part of the complex refractive index of the superstrate, in contrast to the planar waveguide surface plasmon resonance device which responds to changes in both the real and imaginary parts of the refractive index. For example, Piraud *et al.*[21,22] have described an electrochemically regenerated chlorine sensor based on a lutetium phthalocyanine coated integrated waveguide structure, Dunphy *et al.*[18,19] have used grating coupled step index slab waveguides to study adsorption of strongly coloured species at electrode surfaces, and Heineman *et al.*[23,25–28] have recently combined electrochemical modulation, selective adsorption into thin coatings, and planar waveguide optical measurements to develop highly sensitive and selective solution phase chemical sensors. In contrast a bare handful of papers describe SPR studies employing waveguide structures, despite the evident potential advantages of this approach. In earlier work Lavers *et al.*[29] described the use of an integrated planar waveguide to study silver electrodes and the adsorption of tetrabutylammonium ions from a mixture of ethylene glycol and water, a choice which was driven by the necessity of matching the refractive index of the superstrate solution to the operating point of this particular waveguide structure (*vide infra*). Around the same time Chinowsky *et al.*[30] reported the use of a gold coated fibre to study the anodic stripping voltammetry of lead and copper. However the experiments were carried out under poorly controlled electrochemical conditions and the full sensitivity of the technique was not realised.

In this paper we present the first detailed account of the use of a gold-coated integrated optical channel waveguide structure specifically designed for combined electrochemical SPR measurements in aqueous solutions. We describe the design and fabrication of the device and the characterisation of the surface sensitivity using the growth and stripping of the surface oxide on gold and the formation of copper UPD layers as model systems. In future work we envisage using this type of device in sensing applications which combine electrochemical control with high sensitivity SPR detection.

Experimental

Fabrication of gold-coated waveguide structures

The planar waveguide structures with integrated gold electrodes, Fig. 1, were fabricated using conventional photolithographic and ion-exchange techniques. 50 mm square polished Pyrex glass wafers were cleaned with Ecoclear (Logitech), deionised water, acetone (Fisher Chemicals Electronic Grade) and finally propan-2-ol (Fisher Chemicals Electronic Grade) for 20 min each with sonication at a temperature of 50 °C. The Pyrex wafer was then cleaned with piranha solution (1:2 mixture of H_2O_2 and H_2SO_4) for 15 min at room temperature. After thoroughly washing with deionised water and drying in a stream of nitrogen gas, followed by baking at 120 °C for 30 min, the wafers were coated with a 200 nm thick film of aluminium and 10 Y-junction waveguide structures with channels 3 μm wide were opened in this film to form a diffusion mask. The coated wafer was then immersed in molten KNO_3 (Fisher Chemicals Analar Grade) at 389 °C for 7.4 h to form single-moded channel waveguides by ion-exchange of K^+ for Na^+ in the exposed areas of the Pyrex. The refractive index of the Pyrex glass is 1.471 and the exchanged regions have an index of 1.4784, at a wavelength of 633 nm. Alignment marks, to enable accurate positioning of subsequent layers, were then etched into the glass using an ion beam etcher before removing the aluminium diffusion mask using Al etch (containing acetic, phosphoric and nitric acids, supplier Laporte) at 50 °C. The glass wafers were then washed with deionised water and dried in a nitrogen gas stream.

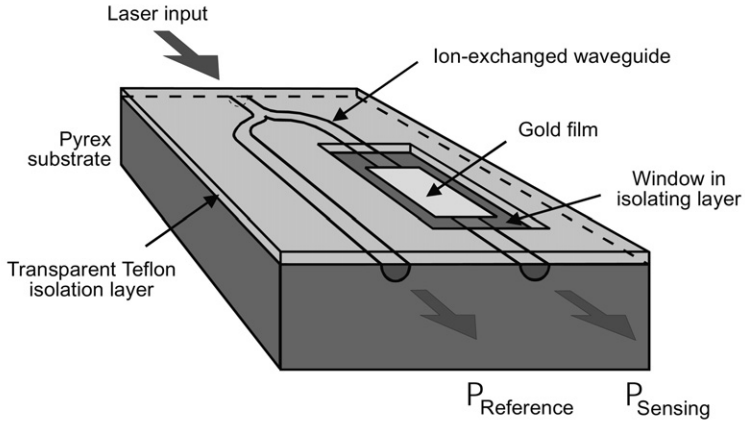

Fig. 1 Diagram of the waveguide surface plasmon resonance structure used in this work.

The edges of the ion-exchanged substrate were chemo-mechanically polished, using Syton (Logitech) to allow efficient end-fire coupling of the incident light into and out of the waveguide. After re-cleaning, the surface of the glass was then treated to promote adhesion of gold by refluxing in a solution of (3-mercaptopropyl) trimethoxysilane (Aldrich) in a water-propan-2-ol (Fisher Chemicals Electronic Grade) mixture (ratio is 1:1:40, by weight) for 15 min.[31] After baking at 100 °C for 15 min a gold film 35 ± 5 nm or 45 ± 5 nm thick was evaporated onto the Pyrex wafer. This gold film was patterned using standard lithographic techniques to produce an array of electrodes each 200 μm wide and between 0.5 and 5 mm long, each located over one arm of a waveguide Y-junction as shown in Fig. 1. The gold films serve both as the working electrode and to guide the surface plasmon. The second, uncoated, waveguide in the Y-junction pair is used to provide a reference output allowing compensation for the effects of input power fluctuations. All electrodes were connected, by a single 15 μm wide track, to 3 mm by 3 mm pads at the edges of the substrate.

Finally a 700 nm thick layer of Teflon AF 1600 ($n \approx 1.31$, Du Pont) was deposited by thermal evaporation on the surface of the substrate and patterned using lift-off to leave windows exposing only the gold electrodes on each Y-junction and the contact pads. This layer helps to isolate the waveguides from the electrochemical cell, which is clamped to the waveguide surface, and from contact with the solution placed in the cell.

This device design has been shown to match the velocity of the surface plasmon wave at the gold surface and the waveguide mode for visible wavelengths at solution refractive indices near that of water. This results in resonant coupling observed as a sharp reduction in output signal power relative to the reference output.[32] The attenuation due to resonant coupling to the surface plasmon may be deduced from the signal/reference output ratio. The configuration of the device allows the strength of the resonant absorption to be adjusted by selection of the length and thickness of the gold-coated electrode region.

Optical and electrochemical measurements

Optical measurements were performed using the apparatus shown in Fig. 2. Light from a 10 mW linearly polarised HeNe laser (Melles Griot) at 632.8 nm was mechanically chopped and passed through a half-wave plate and polariser to select the TM polarisation supported by the surface plasmon. The input power was adjusted using a variable attenuator and the light was end-fire coupled into the waveguide under test using a ×10 microscope objective lens. A ×25 microscope objective lens was used to focus the waveguide outputs onto two silicon photodetectors. The signal and reference powers received, P_S and P_R respectively, were recorded using lock-in detection to remove the influence of ambient light and improve the signal to noise ratio. The measured values were used to calculate the transmittance of the gold coated waveguide, $T = P_S/P_R$.

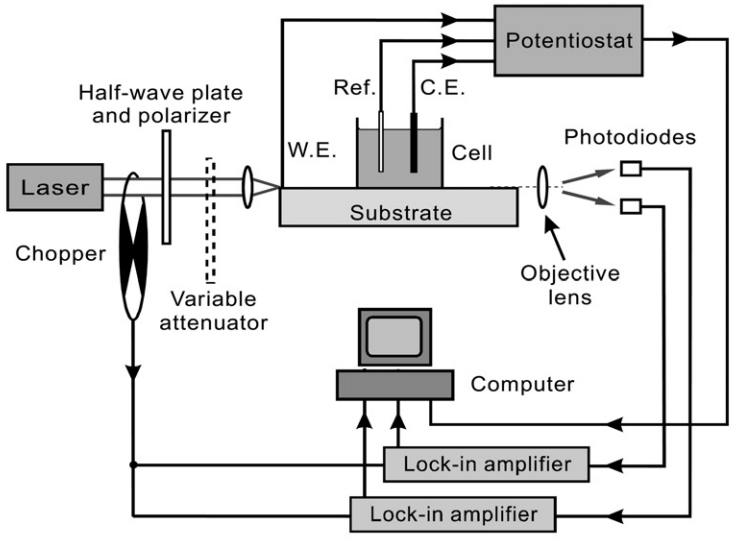

Fig. 2 Schematic representation of the experimental arrangement used to carry out simultaneous electrochemical and transmittance measurements on the waveguide structures.

Two types of liquid cell were used. First, to confirm the response of the waveguide to changes in the refractive index of the bulk analyte, a flow-cell machined from PMMA, clamped to the waveguide surface, and connected to a flow injection analyser was used. Aqueous solutions of sucrose with refractive indices between 1.33 and 1.42 were passed over the waveguide surface and the transmittance, T, measured for each refractive index. The refractive indices of all solutions were measured using an Abbe refractometer at 589 nm.

For the electrochemical measurements, an open silica cell 18 mm in diameter and 13 mm high was clamped to the waveguide surface so that the exposed gold electrode regions of all 10 devices were exposed to the solution. The cell was filled with either 0.2 M sulfuric acid ($n = 1.355$) or 0.1 M perchloric acid ($n = 1.334$). For measurements of the under potential deposition (UPD) of copper, the acid solutions contained 5 mM Cu^{2+} prepared by dissolving the appropriate amount of copper(II) oxide in the acid solution. All electrochemical measurements were made using a three-electrode system with a platinum wire counter electrode and a saturated calomel (SCE) reference electrode. The reference electrode was placed behind a double junction to avoid contamination of the solution by chloride ions. The gold electrode pads were used as the working electrode. No attempt was made to remove oxygen from the solution. The potentiostat and optical measuring equipment was controlled by a single PC running purpose-written code under Labview and equipped with a National Instruments PCI–M10–16XE–10 interface card and a GPIB board.

Results

The waveguide structure

Our integrated waveguide structure consists of a Y-junction bifurcated channel waveguide formed in a Pyrex substrate using photolithographic masking and potassium for sodium ion exchange to produce a gradient index waveguide which is of the order of 10 μm wide. The exchange of K^+ for Na^+ gives rise to a small change in the refractive index of the glass and is a cheap and simple method to produce a single moded waveguide. Gold films of varying length were deposited over one arm of the Y-junction and then a thick transparent Teflon layer was coated over the device leaving only the active area of the gold electrode directly exposed to the superstrate solution, Fig. 1. The Teflon layer serves to define the electroactive area of the electrode and to physically isolate the reference arm of the Y-junction from changes in the refractive index of the superstrate. The Teflon

layer was also found to help protect the device from damage when it was clamped to the base of the electrochemical cell. To achieve high sensitivity of the device to changes in the complex refractive index of the superstrate close to the electrode surface it is essential to design the waveguide structure so that maximum optical attenuation occurs close to the superstrate refractive index. For operation in aqueous solution, at indices between 1.33 and 1.36, the device should be designed with the point of maximum attenuation at a superstrate index of around 1.38. In practice this means that careful thought must be given to the choice of substrate, the refractive index of the waveguiding structure, the thickness and type of the metal layer, and the wavelength of light used to excite the surface plasmon. For experiments in aqueous solution gold is an obvious choice for the metal layer because it supports a surface plasmon in the visible region of the spectrum and is preferable to silver because it is less easily oxidised, even though a less sensitive device results. The waveguide structures were designed using a numerical model for a step index, slab structure.[32] In the simulations the waveguide layer had a depth of 2 μm and a refractive index of 1.4784. The refractive index of the substrate was taken to be 1.4711[33] and the refractive index of the gold at 633 nm was taken to be $0.197 + j3.446$.[34] The model first calculates the mode field distribution of the input waveguide, determines the mode field distributions, velocities and losses of all the guided modes in the gold-coated section, and calculates the distribution of power from the input waveguide to each of these modes. It then allows these modes to propagate over the length of the gold-coated section and combines them, taking their relative phases and attenuations into account, in the output waveguide (which has the same field distribution as the input waveguide). The output power is then normalised to the input power, resulting in the transmittance of the device. Fig. 3 shows the result of a typical calculation for one of our devices, at a wavelength of 633 nm, where the gold film length has been taken to be 1 mm and its thickness 35 nm. Inset is a logarithmic plot of the same data, showing the full depth of the resonance. We believe that the small discontinuity in the slope of the curve on the high-index side of the resonance is due to the model neglecting leaky modes. However, this occurs at a point of very high attenuation, where the device would not be operated. From the figure we can see that the transmittance of the integrated structure, defined as the ratio of the power output from the sensing arm, P_S, divided by the power output from the reference arm, P_R, has a minimum value when the superstrate index is 1.38 and increases rapidly as the superstrate index changes from this value. The minimum in the transmittance curve may be

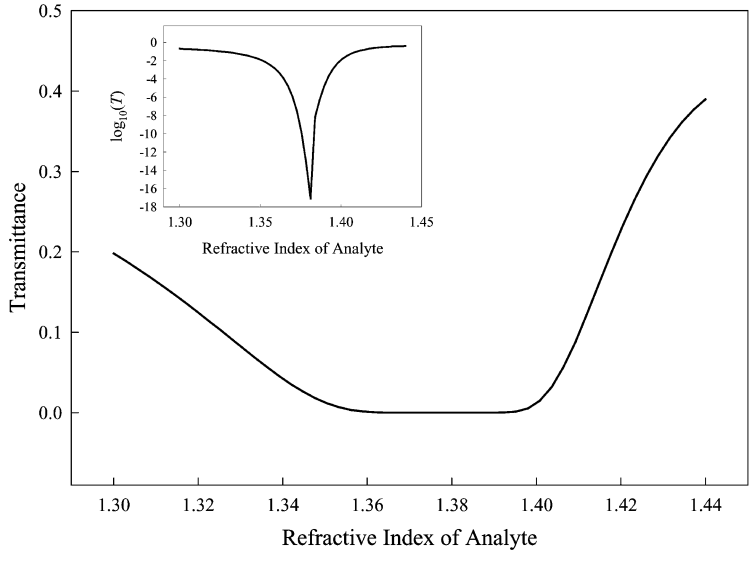

Fig. 3 Calculated profile of transmittance as a function of superstrate refractive index for the waveguide SPR structure shown in Fig. 1. The calculations were carried out assuming a device with a gold film of thickness 35 nm and length 1 mm.

considered to occur when the wavevector of the TM-polarized light propagating in the waveguide matches the wavevector of the surface plasmon wave in the gold. Under these circumstances the maximum amount of power is coupled into the very lossy surface plasmon wave and the power emerging from the sensing arm of the waveguide is at a minimum. Operation at the minimum of transmission is not desirable as, for any reasonable input power, the transmitted power would be low compared with receiver noise. The design must be chosen to maximise the signal-to-noise ratio for a particular configuration. However, Fig. 3 illustrates the importance of careful waveguide design in order to match the performance of the waveguide to the superstrate medium since the resonance covers a narrow range of indices.

Fig. 4(a) shows the experimentally determined transmittance curve for a device with a 3 mm long 35 ± 5 nm thick gold film, as a function of the refractive index of the superstrate. It is clear that although the general shape of the experimental curve is similar to the calculated curve shown in Fig. 3, the quantitative data do not match well. In practice, our waveguides are somewhat different from the simple computational model because they are channel waveguide structures and because

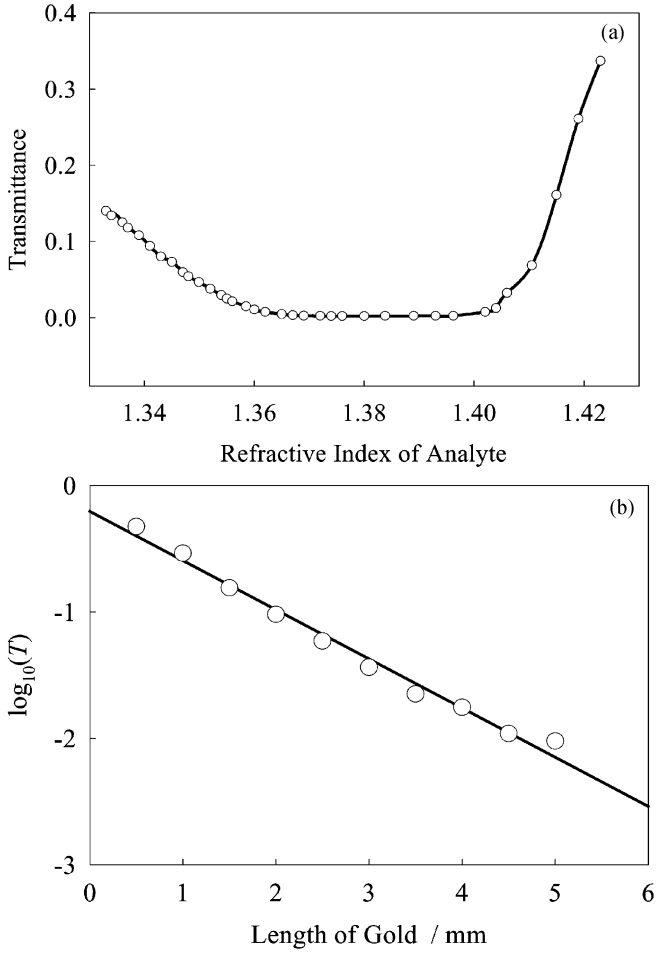

Fig. 4 (a) Plot of transmittance as a function of the superstrate refractive index for a waveguide SPR device with a 35 nm thick gold electrode, length 3 mm and width 200 (m in contact with aqueous sucrose solutions of different concentration. The transmission minimum occurs at a refractive index of 1.376. (b) A plot of the transmittance as a function of the gold electrode length for a set of waveguide SPR devices in contact with water (refractive index 1.33).

there is a gradation in the refractive index introduced by the ion exchange process. Both these factors will cause weaker coupling to the surface plasmon in experimental devices when compared with those modeled using a homogeneous slab waveguide approximation, resulting in practical devices requiring longer gold-coated regions to obtain the same level of attenuation. By an appropriate choice of sensitivity criteria, theoretical sensor designs optimised for a particular task can be generated. The broad minimum in the response shown in Fig. 4(a) exhibits the very high absorption obtained in this index range. It does not necessarily mean that the sensitivity of the device will be low in this region, as this depends upon noise sources. However, in practice, the detection limit for changes in optical power is usually set by fluctuations in spurious radiation scattered in the substrate, which also places a minimum on the transmittance below which measurements cannot readily be made.

The transmittance of the device also depends on the length of the gold electrode. Fig. 4(b) shows a plot of the transmittance for waveguide SPR devices, with gold thickness 45 ± 5 nm, in contact with water (refractive index 1.33) as a function of the length of the gold electrode. As expected from the model, the transmittance decreases exponentially with increasing electrode length, as more of the light propagating in the waveguide is coupled out into the lossy surface plasmon. The length of the gold film can be used as a convenient parameter to adjust the sensitivity of the device.

Electrochemical studies of gold in acid solution

Fig. 5 shows simultaneously recorded electrochemical and optical responses for the waveguide SPR device in 0.2 mol dm^{-3} sulfuric acid solution. The response shown is that obtained after several cycles and is stable under repeated cycling under these conditions. It is immediately obvious that on cycling the electrode potential there are very large changes in the transmittance (it changes by a factor of 4 on cycling from 0.5 V to 1.59 V), that the device can readily detect oxide formation, and that the changes are reversible. Similar measurements on replicate devices and for electrodes of different length (not shown) confirm that these responses are reproducible from one device to another.[35]

The electrochemistry of single crystal and polycrystalline gold electrodes in acid solution has been extensively studied in the literature using cyclic voltammetry alone[36–38] or in combination with other techniques such as the electrochemical quartz crystal microbalance.[9,39,40] The optical responses measured for our waveguide structure have a similar potential dependence to the changes in electroreflectance[40,41] or ellipsometric parameters[7,42,43] reported in the literature for gold electrodes in acid solution. Our waveguide SPR results are also consistent with other reported SPR

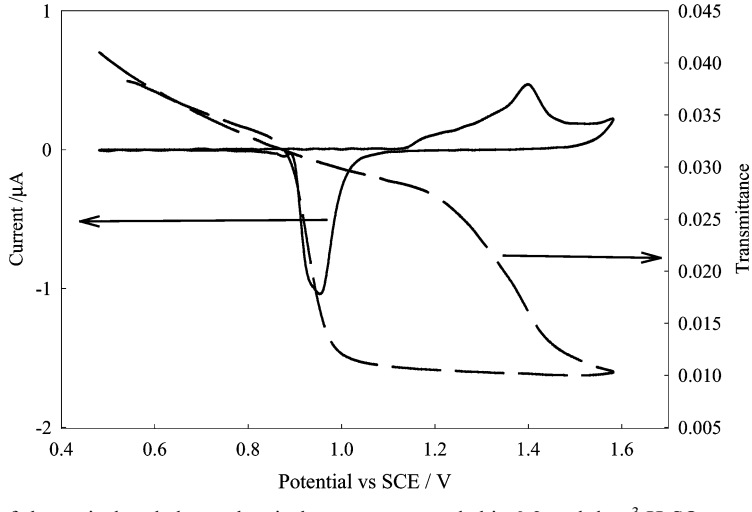

Fig. 5 Plot of the optical and electrochemical responses recorded in 0.2 mol dm^{-3} H_2SO_4 recorded at a scan rate of 20 mV s^{-1}. The length of the gold electrode was 3 mm and its total geometric area was 0.055 cm^2.

studies carried out using the Kretschmann configuration to measure the resonant angle.[7,10,15,16,30] From these studies a common consensus model emerges. Between 0.5 V and 1.13 V on the anodic scan the voltammetry of the polycrystalline electrode is essentially featureless with only double layer charging and, for bisulfate/sulfate anion some evidence for specific adsorption, at least for single crystal electrodes.[37] At 1.13 V, oxidation at the gold surface starts first by adsorption of OH in between the overlayer of adsorbed anions[37] or at step edges.[37] This is followed, at more negative potentials, by a replacement turnover or place-exchange process, driven by repulsion between adjacent Au–O dipoles, leading to the formation of a two-atom thick surface oxide layer. There has been some discussion in the literature as to whether this place-exchange occurs on transfer of the first electron to form AuOH[36,37] or only with the transfer of the second electron. Based on electrochemical quartz crystal microbalance studies, Bruckenstein and Shay[39] have proposed the following mechanism

$$\text{Au-}(H_2O)_{ads} \rightarrow \text{Au-OH} + H^+ + e \quad (1)$$

followed in the second step by

$$\text{Au-OH} \rightarrow \text{Au=O} + H^+ + e \quad (2)$$

$$\text{Au=O} + H_2O \rightarrow \text{O=Au-}(H_2O)_{ads} \quad (3)$$

where the last step represents the replacement turnover process and occurs simultaneously with the transfer of the second electron. Looking at the optical response in Fig. 5, our data support the Bruckenstein and Shay interpretation since the decrease in transmittance associated with the oxidation of the gold surface only commences around 1.23 V, about 0.1 V anodic of the onset of the oxidation current. Following the peak in the oxidation current at 1.4 V and completion of the surface oxide layer the optical response levels off. At more anodic potentials the oxidation current increases again with the onset of oxygen evolution but it is noticeable that the optical response is insensitive to this, indicating the strong surface sensitivity of the technique. On the reverse scan there is a slight increase in transmittance until 1.1 V, at which point the oxide film is stripped from the gold electrode surface and the transmittance increases rapidly, returning to essentially the same value as recorded on the anodic scan. Between 0.87 V and 0.5 V on the cathodic scan the transmittance then increases steadily following the values recorded on the anodic scan.

Fig. 6 shows the corresponding transmittance and cyclic voltammetry data for an experiment carried out in 0.1 mol dm^{-3} perchloric acid. Although there are shifts in the potentials for the oxide formation and stripping processes which can be attributed to the effects of anion adsorption[37] and

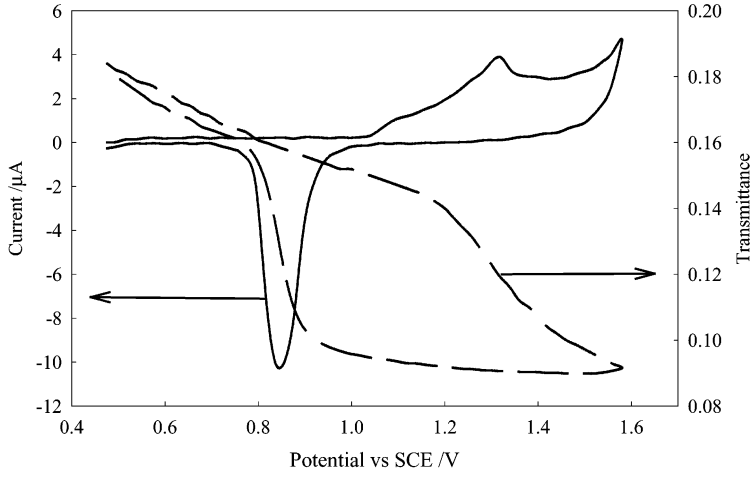

Fig. 6 Plot of the optical transmittance and electrochemical response recorded in 0.1 mol dm^{-3} $HClO_4$ recorded at a scan rate of 20 mV s^{-1} for a gold electrode of length 3 mm.

differences in pH, the results show exactly the same features as seen for sulfuric acid. The most significant difference between the data recorded in 0.2 mol dm^{-3} sulfuric acid (Fig. 5) and 0.1 mol dm^{-3} perchloric acid (Fig. 6) is that the transmittance at 0.5 V in perchloric acid is significantly larger than for sulfuric acid (0.18 rather than 0.04) and that the change in transmittance on formation of the oxide film is proportionally greater for sulfuric acid (a factor of 3 as compared to a factor of 1.7). The difference in the transmittance of the device when in contact with the two solutions arises because of the difference in the refractive indices of the two solutions (1.355 for 0.2 mol dm^{-3}sulfuric acid and 1.334 for 0.1 mol dm^{-3} perchloric acid). As a result, the device is operating at different points on the transmittance/refractive index curve and, as we can see from Fig. 4(a), the transmittance is larger at the lower refractive index. Our model for the waveguide structure[32] predicts that the fractional change on growth of the oxide layer will be smaller in the higher index solution. The experimental data in Fig. 5 and 6 show that the change in transmission at 1.1 V due to formation of the oxide layer is 66% for sulfuric acid and 40% for perchloric acid. The SPR curves for the device both with and without a gold oxide layer have been calculated using our model with a 1 mm long gold electrode for both sulfuric and perchloric acid solutions. The model predicts that the percentage change in the transmission for sulfuric acid should be 97% and for perchloric acid, 67%. The experimental observation that the change in transmission is smaller for the perchloric acid solution than for the sulfuric acid solution is consistent with this prediction, although the percentage changes are higher in both cases. This again highlights the importance of careful design of the waveguide SPR structure if one wishes to achieve maximum sensitivity for a particular application.

We now turn to the double layer region, between 0.5 V and about 1.2 V on the anodic sweep, where the gold surface is not covered by oxide. From the literature[44] we know that the potential of zero charge for the gold electrode in both sulfuric acid and perchloric acid is significantly cathodic of 0.5 V *vs*. SCE so that the decrease in transmittance with increasing anodic potential in this region could be attributed to contributions from the adsorption of anions in the double layer at the electrode surface and from changes in the electron density at the gold surface with surface charge.[8,9,45,46] It is known from the literature that bisulfate/sulfate is the most adsorbing and perchlorate the least absorbing anion at the gold surface.[37] Comparison of our results for sulfuric acid (Fig. 5) and perchloric acid (Fig. 6) shows that the changes in transmittance occurring in the double layer region are almost identical once one takes account of the difference in bulk refractive index for the two solutions, strongly indicating that adsorption of the anion is not the primary cause of the transmittance changes.

According to the model proposed by Hansen[47] and developed by McIntyre[46] to describe electroreflectance, changes in the electrode potential in the double layer region cause changes in the free-electron concentration at the surface of the gold which, in turn alter the dielectric constant for the metal over a layer of thickness of the order of the Thomas–Fermi screening length (about 0.06 nm for gold). If we write the relative permittivity for the metal surface layer, $\hat{\varepsilon}_S$, in terms of the contributions from the free and the bound electrons

$$\hat{\varepsilon}_S = \hat{\varepsilon}_{S,free} + \hat{\varepsilon}_{S,bound} - 1 \tag{4}$$

and assume that the bound electrons do not respond to the applied field, then only $\hat{\varepsilon}_{S,free}$ will change with electrode potential. The magnitude of the change in $\varepsilon_{S,free}$ can be estimated using the Drude equation for a free electron gas[46,48] to give

$$\Delta\hat{\varepsilon}_s = (\hat{\varepsilon}_{bulk} - 1)(\Delta N/N) \tag{5}$$

where $\Delta\hat{\varepsilon}_S$ is the change in the relative permittivity of the surface from the bulk value, $\hat{\varepsilon}_{bulk}$, N is the bulk free electron density and ΔN the change in free electron density in the surface layer. Finally the ratio $\Delta N/N$ can be related to the charge on the electrode surface by

$$(\Delta N/N) = \left(\frac{C_{DL}}{Ned}\right)(E - E_{pzc}) \tag{6}$$

where C_{DL} is the double layer capacitance, e the charge on the electron, d the layer thickness and E_{pzc} the potential of zero charge. This model was used by Kötz *et al.* to explain the shift in the SPR resonance of a gold electrode in contact with 0.5 M $NaClO_4$ solution. In their experiments they

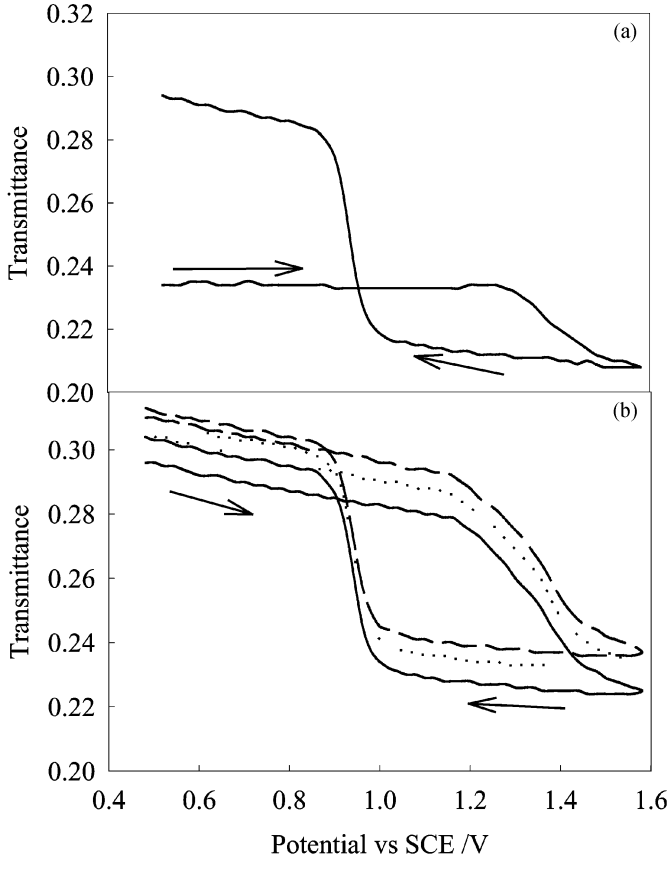

Fig. 7 Plot of the optical transmittance as a function of electrode potential, recorded on (a) the first cycle and (b) the second to fourth cycles, for the waveguide device having a 3 mm long gold electrode, in 0.2 mol dm^{-3} H_2SO_4 cycled at 20 mV s^{-1}.

found a -13 meV V^{-1} shift in the surface plasmon excitation energy in the double layer region at potentials positive of pzc. We have modeled the effects of changes in free electron density upon predicted device transmittance, replacing the top 0.06 nm of the gold film with a film of relative permittivity given by that of gold modified by eqn. (5). The change in transmission due to electron density effects, predicted using this model, for a change in potential of 1 V using the typical value of 0.2 for $\Delta N/N$ is of the order of 2%, significantly less than the experimentally observed value.

The results presented so far have been for the steady state optical and electrochemical responses observed for our devices after repeated cycling for 10 or more cycles. We now briefly describe the changes observed over the first few cycles. On the first cycle using a new device, we observe a lower initial transmittance at 0.5 V which is significantly increased on the return scan, Fig. 7(a). Associated with this we observe a much larger oxidation current at 1.3 V on the first scan. We believe that this effect is associated with the oxidation and removal of organic impurities from the electrode surface. For the second and subsequent scans, Fig. 7(b), the transmittance changes much less and gradually settles down to the steady state behavior described above.

Studies of copper UPD

We have also studied the effects of copper UPD[49–51] using our waveguide devices. Fig. 8 shows the simultaneously recorded steady state cyclic voltammetry and transmittance data recorded in 0.1

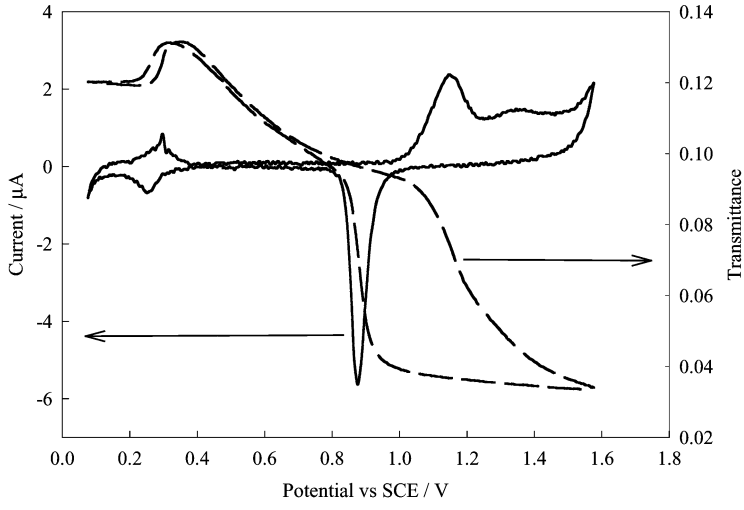

Fig. 8 Plot of the optical transmittance and electrochemical response recorded in 0.1 mol dm^{-3} $HClO_4$ containing 1 mmol dm^{-3} Cu^{2+} recorded at a scan rate of 5 mV s^{-1}. The length of the gold electrode was 3 mm.

mol dm^{-3} perchloric acid containing 1 mmol dm^{-3} Cu^{2+}. Essentially similar results were found in 0.2 mol dm^{-3} sulfuric acid. For these experiments we find that it is necessary to sweep the potential to 1.6 V in order to clean the electrode surface before we can obtain well resolved changes corresponding to the copper UPD at around 0.25 V. Again we find good stability and reproducibility for the optical response of our device. The changes in transmittance associated with the deposition and removal of the copper UPD layer are easily measurable and are reversible. It is also noticeable that at cathodic potentials, when the gold surface is covered by the copper UPD layer, the transmittance is much less potential dependent than in the double layer region. Separate experiments (not shown) confirm that in the absence of the copper UPD layer the transmittance of the device remains potential dependent in this region.[35] These changes in transmittance for the deposition of the UPD layer are quite large when compared to the percentage changes observed using electroreflectance[52,53] or ellipsometry[54] again indicating the high surface sensitivity of SPR. The origin of the observed changes in the electroreflectance for gold following the deposition of a copper UPD layer have been discussed by Kolb *et al.*[53] who concluded that the changes were again due to changes in the free electron density at the gold surface caused by the partially ionic character of the adatoms rather than the effects of absorption of light by the copper monolayer. If this is the case, this explains the effect of formation of the copper UPD layer in the SPR experiment and also why the change in the transmittance with potential is so much less for the copper covered surface than for the bare gold surface if, for the copper covered surface, the copper adatoms determine the free electron density in the gold surface layer. The theoretical model of the device shows that when a layer of copper with a thickness comparable to that of a monolayer of copper (0.75 nm) and a refractive index taken to be $0.27 + j3.4$ [54] is added to the gold surface, the drop in transmission is approximately 10%. This agrees well with the measured change in transmittance of the device upon deposition of a copper monolayer as shown in Fig. 8.

Conclusions

In this work we have demonstrated, for the first time, the use of a channel waveguide surface plasmon resonance structure to make simultaneous electrochemical and SPR measurements at gold electrode surfaces. We have shown that the responses are stable and reproducible and that the technique is especially sensitive to changes occurring at the electrode surface, by demonstrating the significant changes in transmittance of the device following the formation and removal of the surface oxide layer at gold or the formation and removal of a UPD layer of copper. Our studies

emphasize the importance of careful design of the waveguide structure in order that it is matched to the superstrate refractive index in order to maximize the sensitivity of the device.

The combination of electrochemistry and integrated optics offers significant possibilities for future development. The small size (typically 1 mm long by a few μm across) of the sensing region and the ability to fabricate multiple sensing regions on a single substrate using lithographic techniques offers the possibility of building integrated arrays of these devices. By selective modification of the surfaces of the gold electrodes it should then be possible to develop these arrays for use as chemical sensors making direct use of the high surface sensitivity of the SPR measurement combined with electrochemical control and modulation of surface reactions.

Acknowledgement

The authors would like to thank Dr B. Gollas for advice on instrumentation. The Optoelectronics Research Centre is an Interdisciplinary Research Centre supported by the EPSRC. This work was supported in part by EPSRC Grant GR/N26197/01.

References

1 E. Kretschmann and H. Raether, *Z. Naturforsch. A*, 1968, 2135.
2 L. Häussling, H. Ringsdorf, F.-J. Schmidt and W. Knoll, *Langmuir*, 1991, **7**, 1837.
3 A. G. Frutos and R. M. Corn, *Anal. Chem.*, 1998, **70**, 449A.
4 H. J. M. Kreuwel, P. V. Lambeck, J. M. M. Beltman and Th. J. A. Popma, *Proceedings of the 4th European Conference on Integrated Optics*, ed. C. D. W. Wilkinson and J. Lamb, University of Glasgow, 1987, p. 217.
5 S. Löfås, M. Malmqvist, I. Rönnberg, E. Stenberg, B. Liedberg and I. Lundström, *Sens. Actuators, B*, 1991, **5**, 79.
6 M. Malmqvist, *Nature*, 1993, **361**, 186.
7 F. Chao, M. Costa, A. Tadjeddine, F. Abelès, T. Lopez-Rios and M.-L. Theye, *J. Electroanal. Chem.*, 1977, **83**, 65.
8 R. Kötz, D. M. Kolb and J. K. Sass, *Surf. Sci.*, 1977, **69**, 359.
9 J. G. Gordon and S. Ernst, *Surf. Sci.*, 1980, **101**, 499.
10 Y. Iwasaki, T. Horiuchi, M. Morita and O. Niwa, *Electroanalysis*, 1997, **9**, 1239.
11 Y. Iwasaki, T. Horiuchi, M. Morita and O. Niwa, *Sens. Actuators, B*, 1998, **50**, 145.
12 Y. Iwasaki, T. Horiuchi, M. Morita and O. Niwa, *Surf. Sci.*, 1999, **428**, 195.
13 V. Chegel, O. Raitman, E. Katz, R. Gabai and I. Willner, *Chem. Commun.*, 2001, 883.
14 S. Koide, Y. Iwasaki, T. Horiuchi, O. Niwa, E. Tamiya and K. Yokoyama, *Chem. Commun.*, 2000, 741.
15 A. Tadjeddine, D. M. Kolb and R. Kötz, *Surf. Sci.*, 1980, **101**, 277.
16 A. Tadjeddine and A. Hadjadj, *J. Electroanal. Chem.*, 1988, **246**, 43.
17 K. Itoh and A. Fujishima, *J. Phys. Chem.*, 1988, **92**, 7043.
18 D. R. Dunphy, S. B. Mendes, S. S. Saavedra and N. R. Armstrong, *Anal. Chem.*, 1997, **69**, 3086.
19 D. R. Dunphy, S. B. Mendes, S. S. Saavedra and N. R. Armstrong, in *Interfacial Electrochemistry, Theory, Experiment and Applications*, ed. A. Wieckowski, Marcel Dekker, New York, 1999, pp. 513–526.
20 S. S. Saavedra and W. M. Reichert, *Anal. Chem.*, 1990, **62**, 2251.
21 C. Piraud, E. K. Mwarania, J. Yao, K. O'Dwyer, D. J. Schiffrin and J. S. Wilkinson, *J. Lightwave Technol.*, 1992, **10**, 693.
22 C. Piraud, E. Mwarania, G. Wylangowski, J. S. Wilkinson, K. O'Dwyer and D. J. Schiffrin, *Anal. Chem.*, 1992, **64**, 651.
23 Y. Shi, A. F. Slaterbeck, C. J. Seliskar and W. R. Heineman, *Anal. Chem.*, 1997, **69**, 3679.
24 B. L. Ramos, G. Nagy and S. J. Choquette, *Electroanalysis*, 2000, **12**, 140.
25 Y. Shi, C. J. Seliskar and W. R. Heineman, *Anal. Chem.*, 1997, **69**, 4819.
26 A. F. Slaterbeck, T. H. Ridgway, C. J. Seliskar and W. R. Heineman, *Anal. Chem.*, 1999, **71**, 1196.
27 A. F. Slaterbeck, M. L. Stegemiller, T. H. Ridgway and W. R. Heineman, *Anal. Chem.*, 2000, **72**, 5567.
28 Z. Hu, A. F. Slaterbeck, C. J. Seliskar, T. H. Ridgway and W. R. Heineman, *Langmuir*, 1999, **15**, 767.
29 C. R. Lavers, R. D. Harris, S. Hao, J. S. Wilkinson, K. O'Dwyer, M. Brust and D. J. Schiffrin, *J. Electroanal. Chem.*, 1995, **387**, 11.
30 T. M. Chinowsky, S. B. Saban and S. S. Yee, *Sens. Actuators, B*, 1996, **35–36**, 37.
31 C. A. Goss, D. H. Charych and M. Majda, *Anal. Chem.*, 1991, **63**, 85.
32 R. D. Harris and J. S. Wilkinson, *Sens. Actuators, B*, 1995, **29**, 261.
33 J. Gortych and D. Hall, *IEEE J. Quantum Electron.*, 1986, **22**, 892.
34 R. Innes and J. Sambles, *J. Phys. F*, 1987, **17**, 277.
35 J. C. Abanulo, PhD Thesis, University of Southampton, 2001.
36 H. Angerstein-Kozlowska, B. E. Conway, A. Hamelin and L. Stoicoviciu, *Electrochim. Acta*, 1986, **31**, 1051.

37 H. Angerstein-Kozlowska, B. E. Conway, A. Hamelin and L. Stoicoviciu, *J. Electroanal. Chem.*, 1987, **228**, 429.
38 H. Angerstein-Kozlowska, B. E. Conway, K. Tellefsen and B. Barnett, *Electrochim. Acta*, 1989, **34**, 1045.
39 S. Bruckenstein and M. Shay, *J. Electroanal. Chem.*, 1985, **188**, 131.
40 M. E. Hwang and D. A. Scherson, *Anal. Chem.*, 1995, **67**, 2415.
41 T. Takamura, K. Takamura, W. Nippe and E. Yeager, *J. Electrochem. Soc.*, 1970, **117**, 626.
42 J. Horkans, B. D. Cahan and E. Yeager, *Surf. Sci.*, 1974, **46**, 1.
43 R. S. Sirohi and M. A. Genshaw, *J. Electrochem. Soc.*, 1969, **116**, 910.
44 A. F. Silva and A. Martins, in *Interfacial Electrochemistry, Theory, Experiment and Applications*, ed. A. Wieckowski, Marcel Dekker, New York, 1999, pp. 449–462.
45 D. M. Kolb, in *UV-Visible Reflectance Spectroscopy*, ed. R. J. Gale, New York, 1988, pp. 87–188.
46 J. D. E. McIntyre, in *Specular Reflection Spectroscopy of the Electrode-Solution Interphase*, ed. P. Delahay and C. Tobias, Wiley, New York, 1973, pp. 61–161.
47 W. N. Hansen and A. Prostak, *Phys. Rev.*, 1968, **174**, 500.
48 D. Kolb and R. Kötz, *Surf. Sci.*, 1977, **64**, 96.
49 J. W. Schultz and D. Dickertmann, *Surf. Sci.*, 1976, **54**, 489.
50 Z. Shi and J. Lipkowski, *J. Electroanal. Chem.*, 1994, **364**, 289.
51 M. Cappadonia, U. Linke, K. M. Robinson, J. Schmidberger and U. Stimming, *J. Electroanal. Chem.*, 1996, **405**, 227.
52 K. Takamura, F. Watanabe and T. Takamura, *Electrochim. Acta*, 1981, **26**, 979.
53 D. Kolb, D. Leutloff and M. Przasnski, *Surf. Sci.*, 1975, **47**, 622.
54 W. Visscher and A. P. Cox, *Electrochim. Acta*, 1992, **37**, 2245.